ACTIVE COMPLIANT FIXTURES FOR NANOMANUFACTURING

Kartik Mangudi Varadarajan
Massachusetts Institute of Technology
Department of Mechanical Engineering
77 Massachusetts Avenue, Room 3-446
Cambridge, MA 02139
Tel: 617-452-4957, mvkartik@mit.edu

Martin L. Culpepper
Massachusetts Institute of Technology
Department of Mechanical Engineering
77 Massachusetts Avenue, Room 3-449b
Cambridge, MA 02139
Tel: 617-452-2359, culpepper@mit.edu

Keywords: Nanomanufacturing, accuracy, repeatability, kinematic coupling, compliant mechanism

1 Introduction

1.1 Summary

The positioning accuracy of kinematic couplings (KCs) is closely linked to manufacturing and assembly tolerances of the balls and grooves. Passive kinematic couplings achieve sub-micron repeatability, yet at best they provide practical accuracy of 10 microns [1]. The contrast between kinematic coupling accuracy and repeatability is shown qualitatively in Fig. 1A. This level of performance is not acceptable for emerging applications in nano-scale research and Nanomanufacturing. We have developed a mechanized kinematic fixture design, Compliant Nano Fixturing, which incorporates precision mechanisms, fixture constraints and actuators/sensors to enable active control of fixtured position to better than 60 nm alignment under closed-loop control. Flexures are used to improve repeatability and active elements are used to enable the fixture to shift the positions/orientations about which it mates, thereby improving alignment accuracy. This is seen in the shift of the CNF's distribution in Fig. 1A.

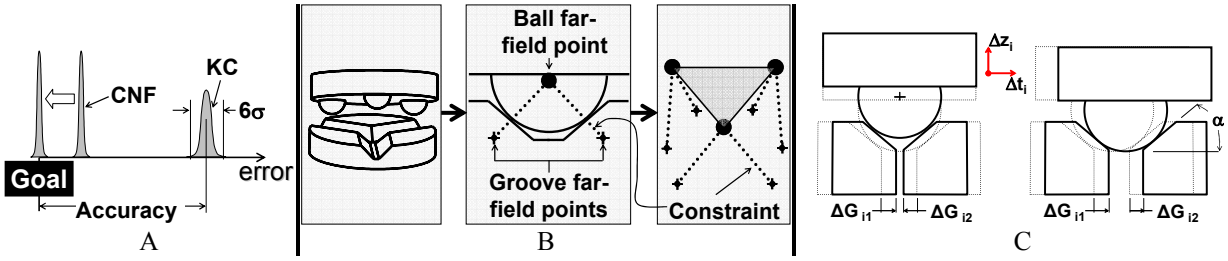

Figure 1: KC alignment characteristics (A), mechanism characteristics (B) and actuated groove design (C)

1.2 Analogy linking kinematic couplings and precision mechanisms

One can think of the constraints between KC balls and grooves as "legs" of a Stewart platform (see Fig. 1B). We see this through a constraint analogy in which the kinematic coupling's ball-groove joints form two constraints. The right side of Fig. 1B shows how the 6 constraints of a KC (2 per ball groove joint x 3 joints per KC) form the constraint profile of a Stewart-Gough platform. From this analogy we can then equate the changing of KC constraints with actuation of a 6 DOF manipulator. Although examples of 2 [2] and 3 [3] axes corrective fixtures exist, we must be able to correct alignment in six axes to achieve tens of nanometer or better positioning. The only existing, 6 axis adjustable coupling, an eccentric ball-shaft design, is limited to micron-level repeatability and accuracy [1] as a consequence of using rolling element bearings. In this paper, we choose to investigate the moving groove design shown in Fig. 1C. The groove surfaces rest upon independent flexure bearings. Through independent actuation of the groove faces, we aim to adjust the fixture in one to six axes with 60 nm resolution.

2 CNF fixture design

2.1 Design concept which uses flexures to guide groove displacement

Figure 2 shows how the grooves, groove flexures and groove plates (to be covered in subsequent sections) are rigidly attached to a monolithic compliant mechanism which contains the six sets of flexure bearings that guide the grooves. Piezo-electric actuators are integrated in the plane of the compliant mechanism such that they are structurally in parallel with their corresponding flexure bearing. The piezo-actuators actuate the flexure-groove-groove plate components in a direction parallel to the plane of coupling. The flexures have been designed so that the overall stiffness (23.7 N/micron in the plane of coupling) is sufficient for most small-scale alignment processes. The KC's balls are pressed into collars which are then pressed into the pallet. It is this pallet which may be use to align parts (attached to the pallet) to many different, grounded mechanized groove components.

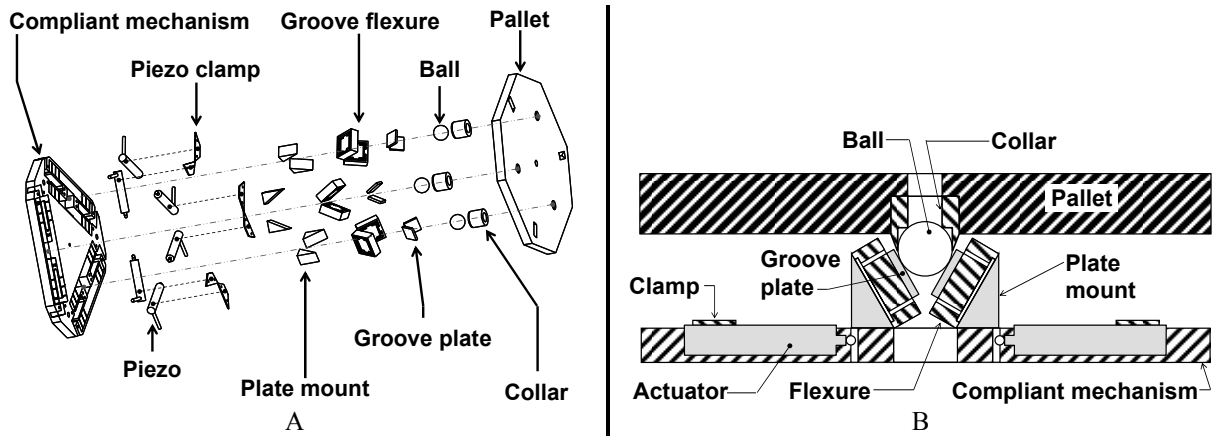

Figure 2: Exploded CNF prototype design (A) and cross-section of ball-groove joint (B)

2.2 Use of flexures in the grooves to limit friction-induced errors and enable mated position adjustments

The performance of kinematic ball-groove fixtures is limited in-part by frictional hysteresis or stick-slip between balls and grooves that slide relative to each other. Flexures can be used to minimize friction-induced errors. In the context of a ball-grove joint, the sliding occurs in two directions:

(1) Into the groove (In the plane of Fig. 2B and parallel to the groove surface): As the coupling engages, the balls slide down into the groove until seated with two points of contact. The friction-induced errors due to this mode of sliding have been addressed by flexures which are placed in grooves such that the ball-groove make contact and then the flexure complies to allow the ball to flex, rather than slide, into a seated position [4].

(2) Along the groove (Into the plane of Fig. 2B): As the balls engage the grooves surfaces, there will be some sliding of the balls along the grooves until the final ball is seated in its groove. The order and amount of ball-groove contact sliding depends on order of ball-groove flat engagement. As a result, variation in order of engagement is a source of coupling error [5]. The CNF design features a groove design which allows engaged or mated ball-groove pairs to move along the groove. This (a) reduces repeatability dependence on order of engagement and (b) enables us to actuate the coupling by changing the groove pattern as shown in Fig. 1C. When this is done, the ball centers must be able to move along the groove to maintain geometric compatibility with the new groove pattern.

The groove flexure shown in Fig. 2 and Fig. 3A was designed to provide stiff constraint in directions (34 N/micron) normal to the ball-groove contacts, and acceptable stiffness (2.13 N/micron) in directions parallel to the groove surface. The flexures were made from 6061 Aluminum and hardened, stainless steel 'groove plates" were bonded to the flexure to provide a contact interface for the hardened stainless steel balls. A parametric stiffness model was formulated for the flexure and then design variables were tailored to achieve a ratio of tangential stiffness to normal stiffness of less than 0.1. The average stiffness of the CNF coupling, in the plane of coupling, was 23.7 N/micron.

2.3 Accuracy/active correction capability

Each groove flexure is mounted upon a corresponding flexure bearing which each consist of six parallel, compliant beams. These guiding flexures can be seen in Fig. 3B adjacent to the flexure grooves (indicated by arrows) and encompassing the piezo-actuators (50µm range, stiffness 20 N/µm). The guiding flexure's stiffness and stress characteristics have been parametrically modeled and optimized to provide an acceptably low stiffness in the actuation direction (1.9 N/µm) and high stiffness in the other directions (440 N/µm normal to actuation direction).

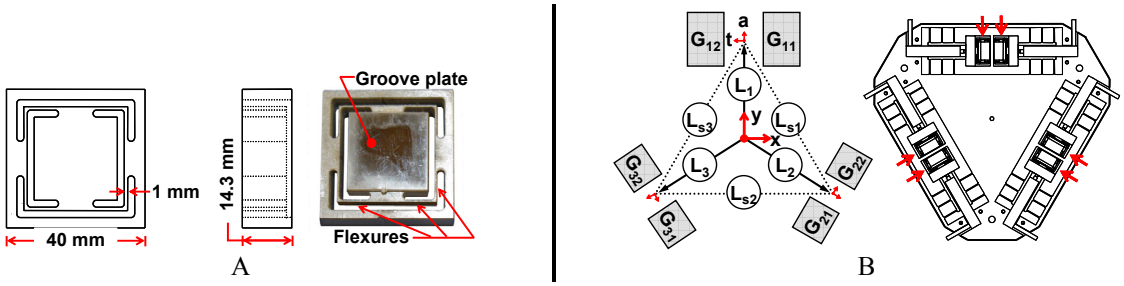

Figure 3: CNF groove flexure design (A) and groove layout (B)

2.4 Kinematic modeling

Figure 3B shows how the grooves are orientated and located with respect to each other by vectors of length L_i. Figure 1C provides examples which illustrate how v-groove i and groove flexure j, may be actuated by an amount ΔG_{ij} to achieve in or out-of-plane motion at a ball-groove joint. Simultaneous in and out-of-plane motion may be achieved by superimposing the in and out-of-plane actuation inputs with different magnitudes. Given the motion of each ball as a function of actuator input, we may then use kinematic solutions for adjustable kinematic couplings [6] to derive equations which describe the fixture's kinematic behavior for the i^{th} groove joint actuation inputs:

$$\Delta g_{i1} = \left(\frac{Z_c - L_i.(\theta_y.c[\theta_i] - \theta_x.s[\theta_i])}{\tan\alpha} \right) + \left(-(X_c - L_i.s[\theta_i].\theta_z).s[\theta_i] + (Y_c + L_i.c[\theta_i].\theta_z).c[\theta_i] \right) \quad (1)$$

$$\Delta g_{i2} = \left(\frac{Z_c - L_i.(\theta_y.c[\theta_i] - \theta_x.s[\theta_i])}{\tan\alpha} \right) - \left(-(X_c - L_i.s[\theta_i].\theta_z).s[\theta_i] + (Y_c + L_i.c[\theta_i].\theta_z).c[\theta_i] \right) \quad (2)$$

3 Experiment

Figure 4A and Fig. B show respectively the grooved and ball-equipped components of the prototype fixture. The majority of the components were waterjet cut from 6061 T6 Aluminum and then machined to add other features. Tests were performed on a thermally isolated, automated test rig, with an air piston applying a 275 N nesting preload through the decoupling flexure shown in Fig. 4C. A dSpace™ data acquisition program controlled the preload engagement for each mating cycle, recorded displacement measurements from six capacitance probes and delivered actuation commands to the piezo-actuators which are then able to drive the coupling with 60 nm resolution.

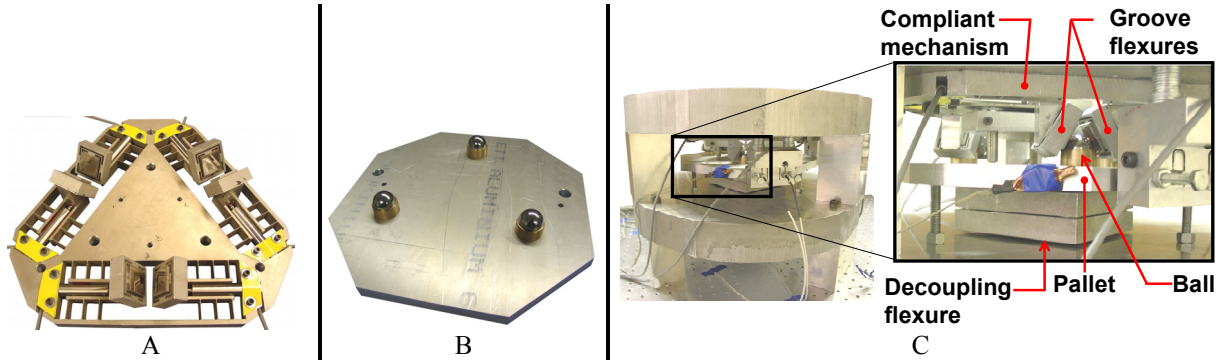

Figure 4: Prototype CNF grooved (A) and ball-equipped component (B) prior to assembly within test rig (C)

4 Discussion of results

Due to page limitations, we may only provide test results which characterize performance in three axes. The plots represent examples of best (y axis) and worst-case (z axis) open loop performance which were measured during the tests. Several test were run in which the fixture was commanded to move in one axis only. The top plots in Fig. 5 show the commanded vs. measured displacement and the middle plots show the off-axis errors. The bottom plots show data from repeated coupling engagement with the piezo-electric actuators receiving a voltage controlled, constant position command.

The worst case, open-loop deviations from desired location were less than 1µm / 20 µradians. This was further reduced through closed loop control to attain better than 60 nm / 2µradians positioning accuracy. This limit is set by the capability of the electronics used to drive the piezo-actuators. If we may depend upon the linearity of the flexure bearings, the mated displacement resolution may be improved to better than 5 nm with improved electronics. The linearity of the plots (no stick slip is evident) indicates that the flexure design allows the ball centers to move along the grooves. Within the parasitic error plots several linear relationships are observable. These are systematic errors that can potentially be reduced through mapping and active adjustment. The waterjet machine which cut the flexures for the fixture was capable of cutting flexure beams with a tolerance of ~ 10% of the flexure beam thickness. As such it is probable that some of these repeatable errors may be due to difference in stiffness between the flexure bearings and differences between the groove flexures. Even so, these are repeatable errors which are a topic of current research aimed at improving the coupling performance through calibration and closed-loop control.

One thousand cycles of engagement and disengagement were performed to characterize the fixture's repeatability characteristics. The ball-groove joints were lubricated with high-pressure grease. The coupling was allowed to settle for 30 seconds before measurements were taken. The test was run over 14 hours. The actuators were supplied with a constant voltage of 2 V. As expected we observe that piezo creep imparts a near-constant rate of transient positioning errors in the Z axis position. The lack of a corresponding, consistent transient trend in the other axes indicates the piezo creep is nearly equal for each piezo-actuator. The difference between the initial (001 – 100 cycles) and settled 1 σ data points (700 – 1000 cycles) of the Y test show less than 50 nm point-to-point difference. This is a strong indicator that little wear or relative sliding motion occurs at the ball-groove interface.

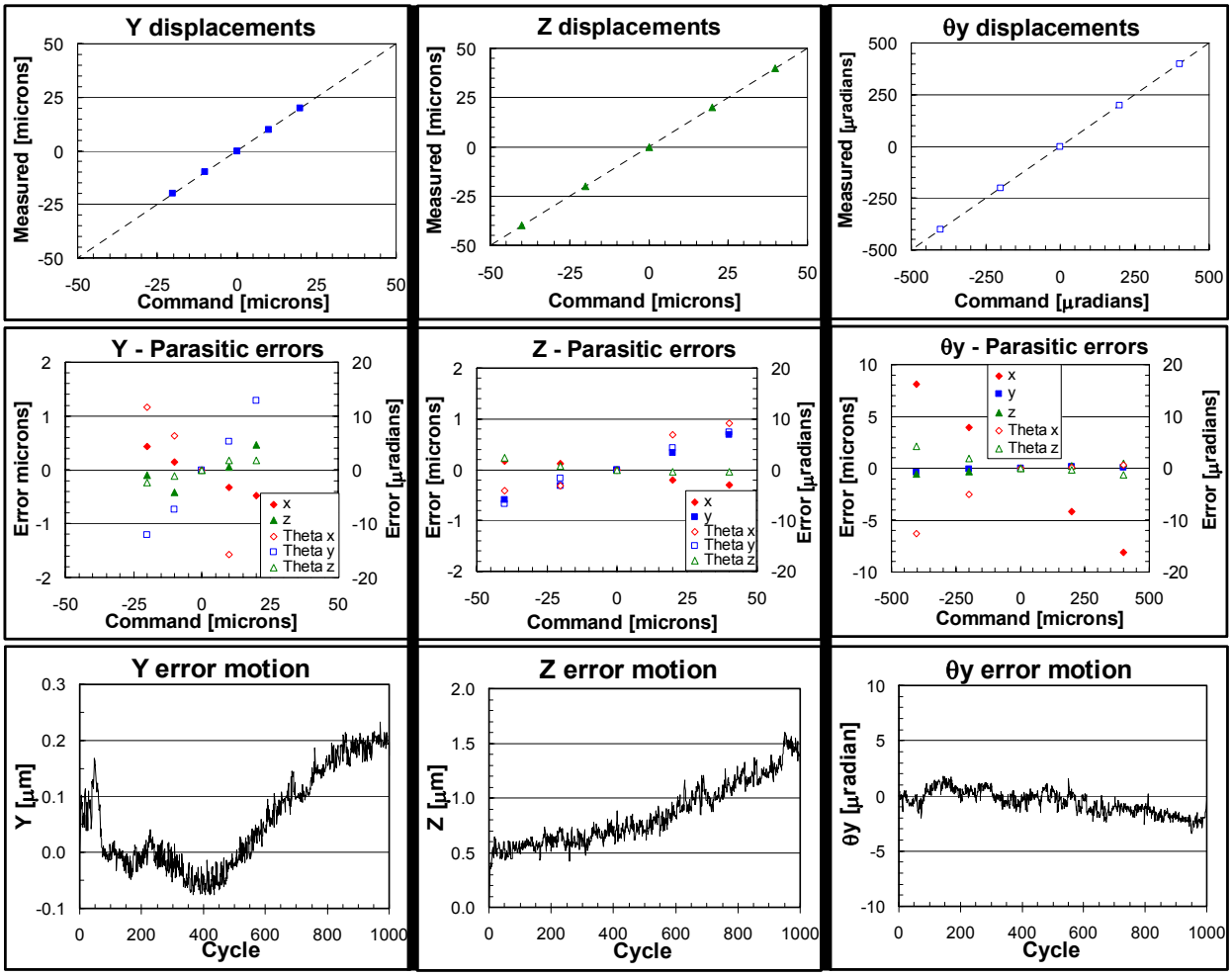

A: In-plane displacement B: Out-of-plane displacement C: Out-of-plane rotation

Figure 5: Open loop experimental results

5 References

[1] Culpepper, ML Mangudi KV, Dibiaso, M, Modeling and design of exact constraint fixtures for micron-level repeatability and accuracy, Accepted for publication in Prec Eng, 2003.

[2] Taylor, JB, and Tu, JF Precision X-Y Microstage with maneuverable kinematic coupling mechanism, Prec Eng, April, 1996, vol. 18, No. 2, p.85 – 94.

[3] Chui, MA, Roadmap of mechanical systems design for the semiconductor automatic test equipment industry, MIT Ph.D. thesis, 1998.

[4] Schouten CH, Rosielle PCJN, Schellekens PHJ. Design of a kinematic coupling for precision applications. Prec Eng;20;46-52.

[5] Hale, LC. and Slocum, AH., Optimal design techniques for kinematic couplings, Prec Eng, April 2001, vol. 25, No. 2, 114-27.

[6] Culpepper, ML, Araque, C, and Rodriguez, M, Design of accurate and repeatable kinematic couplings, Proc of the 2002 Annual Meeting of the American Society for Precision Engineering, October, 2002, pp. 279-84.